Mine Water Environ (2012) 31:344–352
DOI 10.1007/s10230-012-0203-7

TECHNICAL ARTICLE

Mineralogy of Fe-Precipitates and Their Role in Metal Retention from an Acid Mine Drainage Site in India

P. K. Sahoo · S. Tripathy · M. K. Panigrahi · Sk. Md. Equeenuddin

Received: 8 January 2012 / Accepted: 23 August 2012 / Published online: 18 September 2012

Abstract Iron-rich precipitates from acid mine drainage (AMD) sites around the Jaintia Hills coalfield, India, were investigated. The ochreous precipitates mainly consist of schwertmannite, goethite, and jarosite. Sorption affinities suggest that Ni, Mn, Cr, Cd, Pb, and Zn are more significant in schwertmannite-bearing ochre than in more crystalline jarosite- and goethite-bearing ochres. The lower crystallinity and higher surface area of schwertmannite-bearing ochreous precipitate result in higher metal retention potential. Fe and Mn concentrations in water may also influence the sorption of metals in the precipitates. The results of the sequential extractions showed that metal mobility is mainly controlled by Fe and Mn oxyhydroxide phases. This information may aid understanding of the natural attenuation of trace metals by ochreous precipitates in AMD-contaminated water.

P. K. Sahoo (✉)
BK21 Advanced Geo-Environment Research Team,
Department of Environmental Engineering,
Kunsan National University, Gunsan, Jeonbuk 573-701,
Republic of South Korea
e-mail: prafulla.iitkgp@gmail.com

P. K. Sahoo · S. Tripathy (✉) · M. K. Panigrahi ·
Sk. Md. Equeenuddin
Department of Geology and Geophysics, Indian Institute
of Technology, Kharagpur 721302, West Bengal, India
e-mail: stripathy@iitbbs.ac.in

S. Tripathy
School of Earth, Ocean and Climate Sciences,
IIT, Bhubaneswar 751013, India

Sk. Md. Equeenuddin
Department of Mining Engineering, National Institute
of Technology, Rourkela 769008, Odisha, India

Keywords Acid mine drainage · Ochreous precipitates · Mineralogy · Metal · Sequential extraction

Introduction

Acid mine drainage (AMD) generated from coal mines is a significant water quality problem throughout the world (Gammons et al. 2010). It is caused by weathering of sulfides through biogeochemical processes under atmospheric conditions, resulting in acidification of water and the release of Fe^{2+}, SO_4^{2-}, and metals (Kleinmann et al. 1981). The oxidation of Fe^{2+} to Fe^{3+} and subsequent hydrolysis lead to the formation of a variety of poorly ordered to well crystalline Fe oxyhydroxide and/or oxyhydroxysulfate phases (Bigham and Nordstrom 2000). The poorly ordered Fe-precipitates are metastable and can transform to more stable forms depending on geochemical conditions (Burton et al. 2007). These precipitates are of major environmental importance since they regulate the bioavailability and mobility of metals and effectively scavenge them from the aqueous reservoirs (Carlson et al. 2002; Davis and Kent 1990; Lee et al. 2002; Lu et al. 2011). However, their sorption capacity varies based on mineralogy (Sidenko and Sherriff 2005; Webster et al. 1998). Although extensive studies have been carried out on mineralogy and metal enrichment in ochreous precipitates (Acero et al. 2006; Equeenuddin et al. 2010; Kim et al. 2003; Schroth and Parnell 2005; Sidenko and Sherriff 2005; Webster et al. 1998), very limited work has been done on distribution of metals in different geochemical phases of AMD precipitates from coal mines (Kairies et al. 2005). AMD generated from the Jaintia Hills coalfield and its impact on surrounding water quality has been investigated recently by Sahoo et al. (2012) and Swer and Singh

(2003). However, no information is available on the characteristics of ochre precipitates from such highly acidic water. The purpose of this study was to fill this gap through mineralogical characterization of the ochreous precipitates at the AMD impacted sites and evaluation of their metal retention potentials, and to study the geochemical association of metals in the precipitates.

Description of Study Area

The study area is located in Jaintia Hills, Meghalaya, India (Fig. 1), where coal mining started in 1970 using primitive subsurface mining methods, commonly known as 'rat-hole' mining. The type of coal in this area is mostly sub-bituminous in rank and is high (3–5 %) in sulfur (Chandra et al. 1983; Swer and Singh 2003). The coal deposits occur in the Lakadong sandstone of Eocene age, and were deposited in a marine environment (Chandra et al. 1983). This member of the Tertiary Group of rocks contains three persistent coal seams ranging from 0.3 to 1.2 m in thickness. The coal beds contain clay, carbonate, nodules of pyrite, sandstone, pyritic sandstone, and carbonaceous shale (Ahmed and Bora 1981; Singh and Singh 2000; Swer and Singh 2003). Pyrite occurs as disseminated discrete grains, framboids, massive replacements, and fissure fillings (Singh and Singh 2000).

Materials and Methods

Sampling

Waters and ochreous precipitates were collected from AMD affected streams (Fig. 1) around the coalfield during low stream flow. Ochreous precipitates were collected using a clean plastic scoop and then placed in polypropylene vials and immediately sealed. Water samples at ochre sample sites (Fig. 1) were collected in acid-washed HDPE bottles. Water pH was measured in the field, and samples were filtered using 0.45 μm nylon filters and collected in duplicate. The samples were acidified with 4 % suprapure HCl for Fe^{2+} determinations and with HNO_3 for general metal analysis.

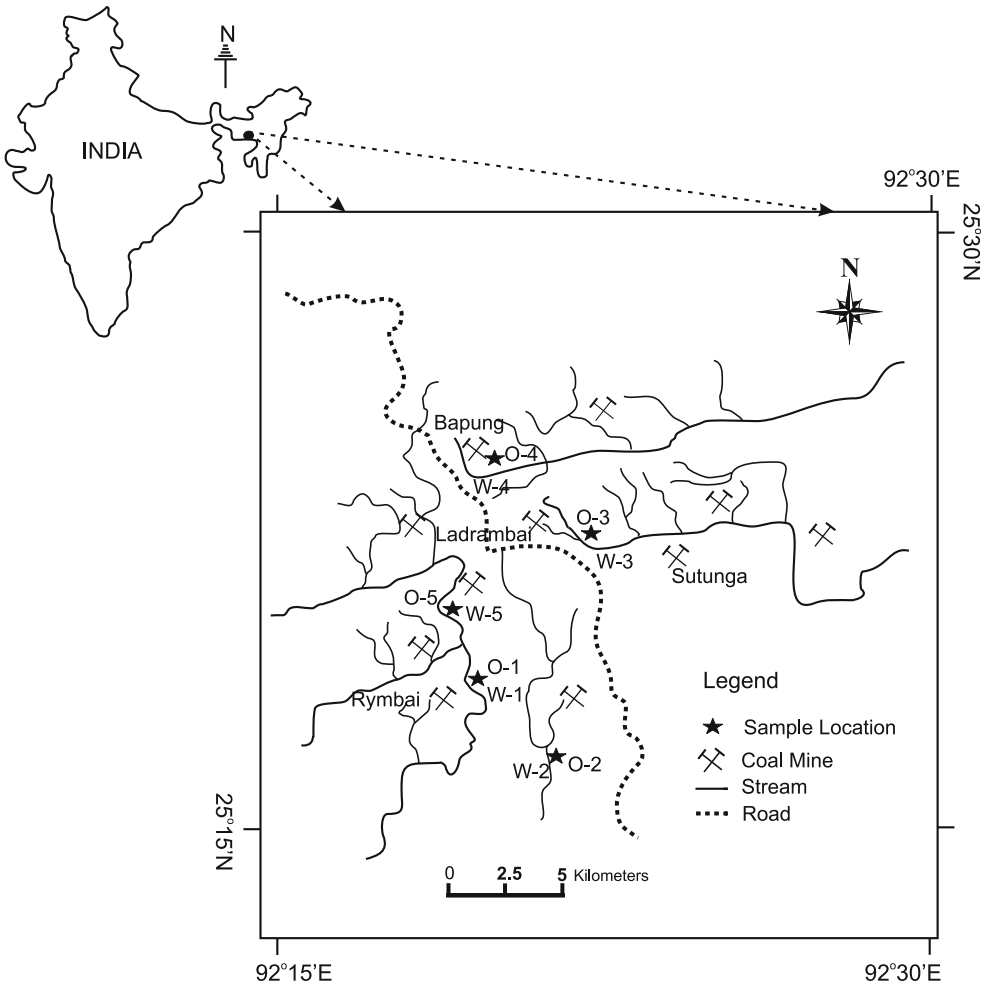

Fig. 1 Study area and sampling locations of ochreous precipitates (*O-1* to *O-5*) and colocated water (*W-1* to *W-5*) samples around the Jaintia Hills coalfield

Laboratory Methods

The precipitates were air dried at room temperature and packed in air-tight polyethylene packets prior to analysis. Their mineralogy was determined on a Philips PW-1710 X-ray diffractometer (XRD) using CuKα radiation. Infrared spectra were obtained using a NEXUS 870 fourier transform infrared spectrometer (FTIR) (Thermo Nicolet) spectrometer. Morphological features of the precipitates were observed using a ZEISS EVO 60 scanning electron microscope (SEM), equipped with an energy dispersive X-ray spectrometer (EDX). The poorly crystalline Fe hydroxides were extracted at a pH of ≈3.0 in the dark using 0.2 M ammonium oxalate (Schwertmann 1964). Total concentrations of Fe, Mn, Ni, Cu, Cr, Pb, Cd, and Zn in the precipitates were determined by digesting the samples in aqua-regia (1:3 HNO_3/HCl) followed by atomic absorption spectrophotometry (AAS) (Perkin Elmer Analyst 300). Total S was measured by EDX. Specific surface area was measured by the B.E.T method following Brunauer et al. (1938).

Sequential extractions were performed using the methods of Kairies (2003). The sequential extractions involved combining one gram of sample with following reagents: deionized water (40 ml, 25 °C, 15 min shaking) for extraction of water soluble components (Step 1); 0.1 M acetic acid (40 ml, 25 °C for 16 h shaking) for extraction exchangeable and carbonate components (Step 2), 0.1 M cold hydroxylamine hydrochloride (40 ml, 25 °C, 16 h shaking) for extraction of Mn oxides and hydroxides (Step 3), 0.25 M hot hydroxylamine hydrochloride in 0.25 M HCl (40 ml, 85 °C, 16 h shaking) for extraction of Fe oxide-hydroxides (Step 4), 30 % H_2O_2 (10 ml, 25 °C, 1 h, 85 °C; added 10 ml more, 1 h 85 °C) followed by 1 M ammonium acetate (50 ml, 16 h) (Step 5) for extraction of organic and residual fractions. The concentrations of metals such as Cd, Cu, Mn, Fe, Zn, Ni, and Pb in the aqueous extracts were measured using AAS. The recovery of metals ranged from 97.4 to 111 % of bulk concentration. Duplicate samples are analyzed at a frequency of one to every three samples to assess the precision of the method. The results were statistically evaluated using Pearson correlation coefficient and descriptive statistics using SPSS 18. The precision was within ±10 % for all metals.

The concentrations of Cd, Cu, Mn, Fe, Zn, Ni, and Pb in water samples were measured using inductively coupled plasma-mass spectrometry (ICP-MS) (Varian 820 MS). The analytical errors were within ±5 % for all metals. Ferrous concentration was determined by the 1,10-phenanthroline colorimetry method at 510 nm while SO_4^{2-} was measured using the barium sulfate turbidimetry method at 420 nm (APHA 1995). The detection limit for both ions was 0.5 mg/L and the precision was better than 5 %. The concentration of Fe^{3+} was obtained by subtracting Fe^{2+} from total Fe.

The ICP-MS method was calibrated using a multi-element stock standard solution of CertiPUR (10 mg/L) and blanks. Working standard solutions with elemental concentrations of 10, 100, and 1,000 µg/L were prepared from stock solution using deionized water and 1 % ultrapure grade nitric acid. For calibration verification, 50 µg/L of multi-element standard solution (CertiPUR) were used. For AAS, standard solutions of individual metals were made from stock solutions (1,000 mg/L, Merck grade) in 1 % ultrapure nitric acid. For calibration verification, 0.5 mg/L of multi-element standard solution (CertiPUR) were used.

Results and Discussion

Mineralogy and Morphology

The principal mineral phases identified in the precipitates using XRD were goethite, schwertmannite, and jarosite along with quartz (Fig. 2). Schwertmannite was identified from its characteristic strongest peak at 2.58 Å as an individual phase or occurring with goethite. Jarosite was identified with considerable amounts of quartz. Goethite was identified alone or together with schwertmannite or jarosite. The corresponding pH values of mine water for jarosite-, goethite-, and schwertmannite- dominated precipitates are 2.5, 2.5–3.7, and 3.3, respectively. The occurrence of these minerals agrees with their theoretically predicted mineralogy based on pH according to Bigham et al. (1996).

Fourier transform infrared spectrometer was also used for the identification of minerals in the ochreous precipitates. In the FTIR spectra of precipitates (Fig. 3), two SO_4 absorption bands due to $v_3(SO_4)$ and $v_4(SO_4)$, are observed at 1,110–1,120 and 601 cm^{-1} respectively. A Fe–O band at 703 cm^{-1} confirmed the presence of schwertmannite (Bigham et al. 1990). The single broad band at 1,110–1,120 cm^{-1} corresponds to the outer-sphere sulfate while the absorption band at 601 cm^{-1} corresponds to structural sulfates located in the tunnel cavities of schwertmannite crystals (Regenspurg and Peiffer 2002). The absorption band at 630 cm^{-1} is due to jarosite (Lazaroff et al. 1982), while those at 890 and 794 cm^{-1} are assigned to the δ-OH and γ-OH bending vibration in goethite according to Cornel and Schwertmannite (1996). The prominent spectra between 3,160 and 3,410 cm^{-1} are due to H_2O-stretching (Murad and Rojik 2003), while the 1,632 cm^{-1} band is due to H_2O bending (Ryskin 1974). The minor bands at 3,620 and 3,697 cm^{-1} are attributed to kaolinite (Murad and Rojik 2003; Saikia and Parthasarathy 2010).

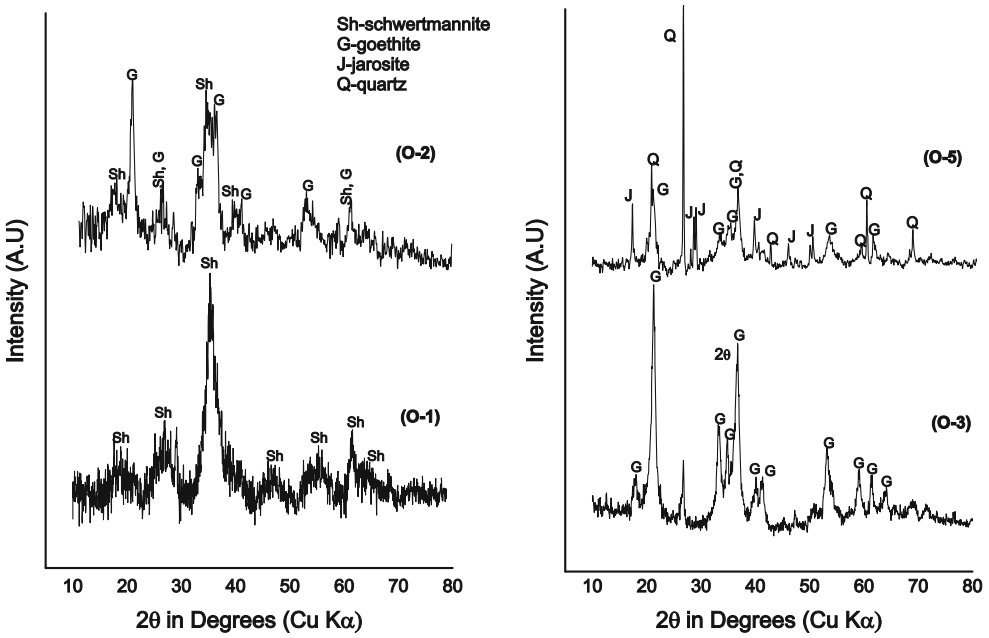

Fig. 2 X-ray diffractogram of ochreous precipitates collected from Jaintia Hills coalfield

Poorly crystalline Fe minerals cannot always be identified by XRD because of the presence of other more crystalline phases such as clay minerals and quartz. Therefore, the ratio of the oxalate extractable Fe (Fe_{ox}) to total Fe (Fe_{tot}) (Table 1) aided in identification. Schwertmannite dissolved completely in the ammonium oxalate solution (pH = 3.0), whereas goethite and jarosite did not. Jarosite-bearing ochres have the lowest Fe_{ox}/Fe_{tot} ratios (0.42), followed by goethite-bearing ochres (0.57), because of their well crystallized nature, while the ratio for mainly schwertmannite-bearing ochre is 0.94 due to its poor crystallinity (Bigham et al. 1990). The Fe_{ox}/Fe_{tot} ratio decreased to 0.68 for a mixture of schwertmannite and goethite compared to 0.57 for pure goethite. This may be attributed to partial transformation of poorly crystalline ochres into more crystalline phases (Jönsson et al. 2005).

The morphology of the minerals was investigated using SEM (Fig. 4). The presence of schwertmannite was confirmed from its spherical pin-cushion morphology (Fig. 4a) with bundles of needles (≈0.1–1 μm in length, ≈0.05 μm in width) coalescing to form rounded aggregates (2–6 μm diameter) (Bigham and Nordstrom 2000). Pseudocubic jarosite crystals (Fig. 4b) (≈10 μm in length) were observed. Goethite was identified by its nodular shape with average diameter ≈30–200 nm (Fig. 4c). If goethite forms from the recrystallization of schwertmannite, goethite may preserve the morphology and size of the original schwertmannite (Fig. 4d) (Jönsson et al. 2005; Schwertmann and Carlson 2005).

Metal Enrichment

The amount of metals partitioned into ochreous precipitates is helpful in evaluating the mobility of metals at this site as well as at similar sites. Concentrations of selected elements determined in the ochreous precipitates are given in Table 2. The average concentrations for all metals, except Mn, are higher than their respective crustal abundances. Furthermore, the concentrations of these metals are low in aqueous samples relative to the corresponding ochres (Table 2) suggesting that Fe-precipitates are effective scavengers of metals. Higher concentrations of these metals, except Cu, are generally associated with schwertmannite-bearing ochres, whereas the lowest concentrations of metals are associated with jarosite-bearing ochre (Fig. 5). This illustrates the control exerted by mineralogy and crystallinity on metal mobility.

Partitioning of metals is generally quantified using distribution of coefficient (K_d). However, this parameter is only useful for specific conditions and systems (Rose and Bianchi-Mosquera 1993), and equilibrium between the water and precipitates cannot be assumed. In comparison, Munk et al. (2002) used a concentration ratio (CR) to discuss the metal distribution, using the same formula for K_d.

$$CR = \frac{X_s}{X_l} \quad (1)$$

where X_s is the concentration of an element in the precipitate and X_l is the aqueous concentration.

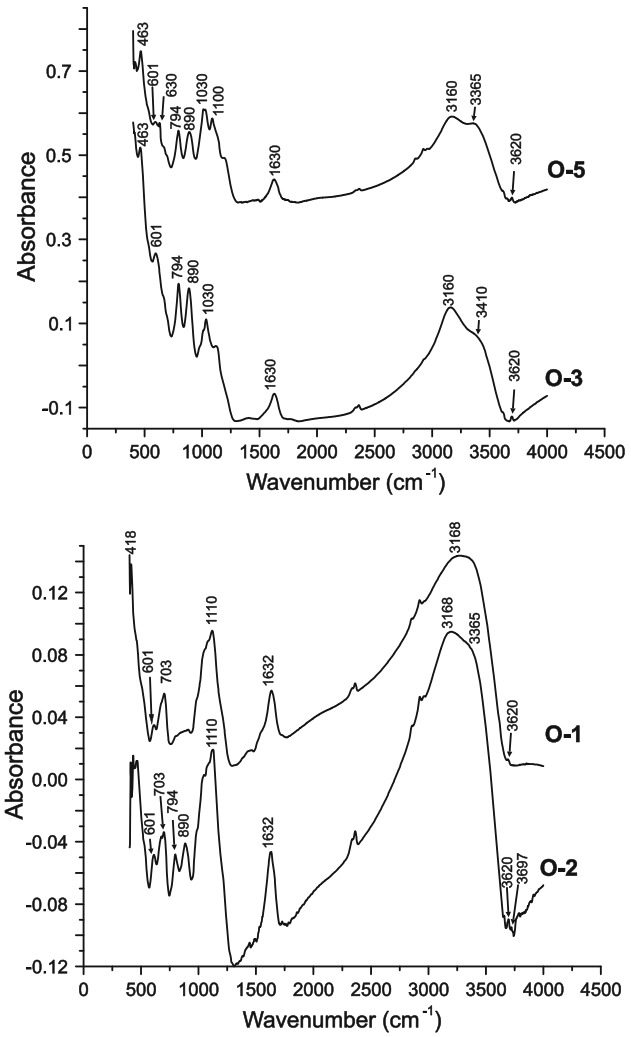

Fig. 3 FTIR spectra of ochreous precipitates collected from AMD affected streams in the Jaintia Hills coalfield

In this study, CR is used to compare precipitate enrichment as well as the distribution of metals between the solid and liquid phases and sorption affinities of metals in the precipitates. From Table 3, it is observed that schwertmannite-bearing ochre has the higher enrichment for Ni, Mn, Cd Cr, Pb, and Zn relative to the associated mine water compared to its well crystalline counterparts (i.e. jarosite and goethite). Although the order of sorption affinity varies between precipitates (Table 3), Cr and Fe had the highest order affinity in all samples, while Mn had the lowest. This result is comparable to experimental and modeled K_d values of metals determined by Dzombak and Morel (1990) on synthetic goethite where Cr had the highest affinity, and the experimental CR values for the goethite surface determined by Kairies et al. (2005) where Mn had the lowest affinity. Cornel and Schwertmannite (1996) also reported the lowest affinity for Mn sorption. Sorption of metals on ochreous precipitates is controlled by surface hydroxyl groups, which are coordinated with Fe (Cornell and Schwertmann 1996). Increasing the number of surface hydroxyl groups on ochre favors more sorption of metals due to their high surface area (Cornel and Schwertmann 1996). The specific surface area of Fe oxyhydroxide precipitates in mining environment is known to vary between 50 and 200 m^2/g (Bigham et al. 1990; Gagliano et al. 2004). In the present study, the surface area ranged from 52 to 147 m^2/g, with schwertmannite having the highest surface area. Schwertmannite also has the highest trace-metal concentrations among all the ochres. The high surface area and poor crystallinity make schwertmannite highly effective at sorbing metals from solution (Xu et al. 1997). If a poorly crystalline precipitate transforms to a more crystalline product or any crystalline product is directly formed, the crystals become larger and surface area and crystal lattice space decrease, leading to fewer surface sorption sites (Kairies et al. 2005). This may decrease sorption, as occurs with jarosite and goethite. The concentration of sulfate in ochre may also influenced the sorption of metals by creating a net negative charge on iron hydroxide surfaces (Ali and Dzombak 1996). It is observed that metal sorption increases with increasing concentrations of sulfate, except in O-5, which may be due to the crystalline nature of this precipitate. Dissolved SO_4^{2-} in the solution may also influence the sorption of trace metals onto the Fe-precipitates by creating a net negative charge at the hydroxyl surface (Ali and Dzombak 1996) or by creating mixed metal–ligand surface complexes (Ali and Dzombak 1996; Webster et al. 1998). However, in the present study, the role of the dissolved SO_4^{2-} was found to

Table 1 Chemical (wt%), physical and mineralogical properties of ochreous precipitates

Sample ID	Mineralogy	pH of water	Fe(tot)	Fe(ox)	Fe(ox)/Fe(tot)	S(%)	SSA(m^2/g)
O-1	Sh	3.3	41.20	38.60	0.95	3.87	147
O-2	G, Sh	3.7	46.30	36.20	0.78	2.45	112
O-3	G	3.1	41.80	23.70	0.57	1.46	87
O-4	Sh, G	3.4	37.40	25.40	0.68	1.88	101
O-5	J, G	2.5	28.20	12.50	0.42	4.52	52

Sh schwertmannite, *G* goethite, *J* jarosite, *Fe(tot)* total Fe, *Fe(ox)* oxalate extraction Fe, *SSA* specific surface area

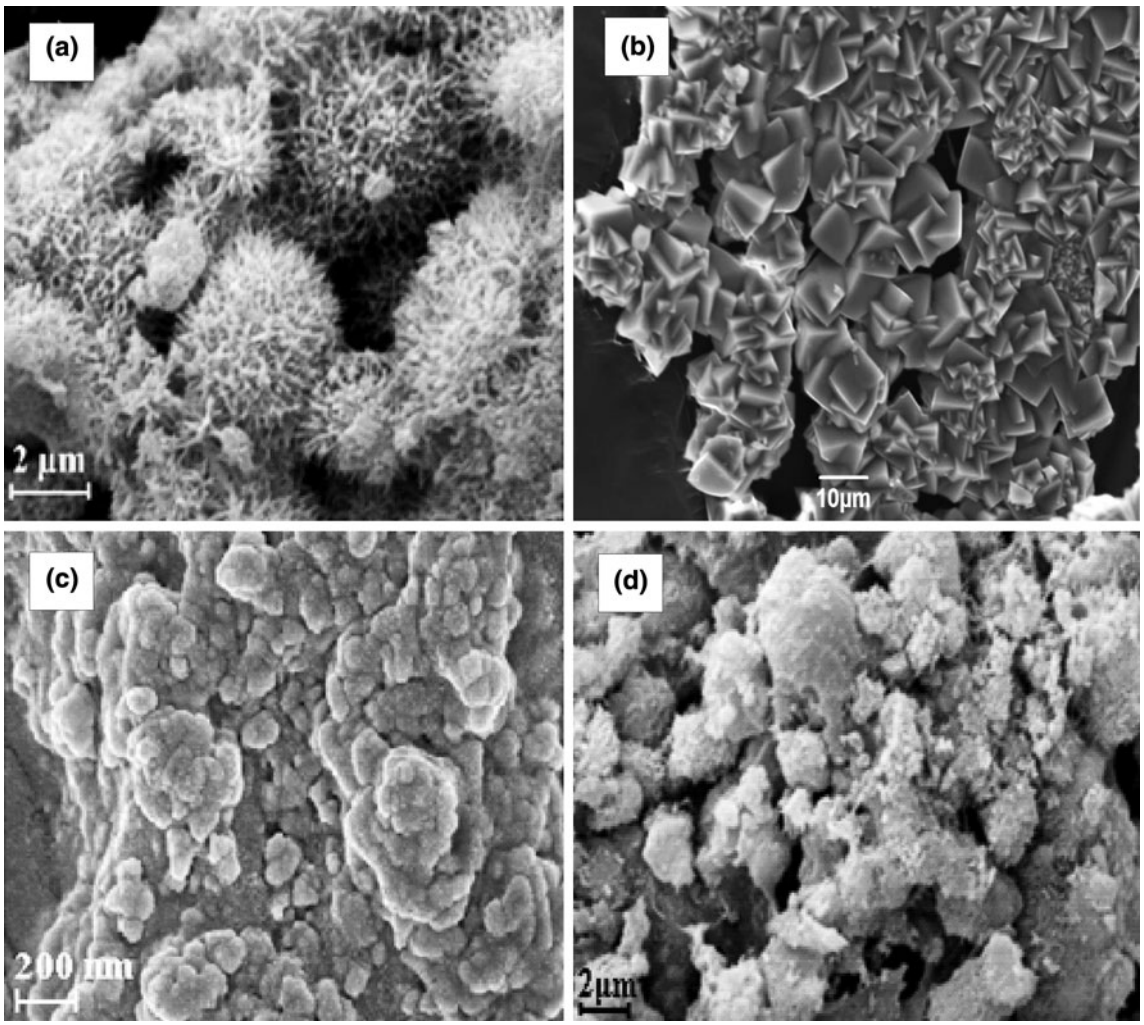

Fig. 4 SEM images of ochreous precipitates **a** schwertmannite, **b** jarosite, **c** goethite, and **d** mixture of schwertmannite and goethite

Table 2 Concentrations of selected elements in ochreous precipitates (O-1–O-5) (mg/kg) and stream waters (W-1–W-5) (mg/L)

Sample ID	Ni	Mn	Zn	Cr	Pb	Cd	Cu	Mineralogy
O-1	285	473	139	276	54.9	7.5	20.6	Sh
O-2	203	203	116	85	36.3	8.7	35.3	G, Sh
O-3	162	141	64	136	18.2	2.5	53.6	G
O-4	127	124	101	215	40.3	3.2	21.2	Sh, G
O-5	51	79	47	52	10.2	0.8	13.4	J, G
AVG	166	204	93	153	32.0	4.5	28.2	
CA[a]	56	716	65	126	14.8	0.1	25.0	

	Ni	Mn	Zn	Cr	Pb	Cd	Cu	Fe(II)	Fe(III)	SO_4^{2-}
W-1	0.034	0.46	0.017	0.002	0.031	0.006	0.006	7.4	24.5	594
W-2	0.047	0.72	0.034	0.002	0.040	0.002	0.002	6.5	15.3	349
W-3	0.125	1.45	0.580	0.003	0.080	0.010	0.020	4.4	16.8	514
W-4	0.040	0.45	0.023	0.004	0.028	0.124	0.003	4.3	28.1	425
W-5	0.350	1.70	0.720	0.006	0.054	0.008	0.050	41.0	18.2	736

AVG average, *CA* crustal abundance, *Sh* schwertmannite, *G* goethite, *J* jarosite

[a] Wedepohl (1995)

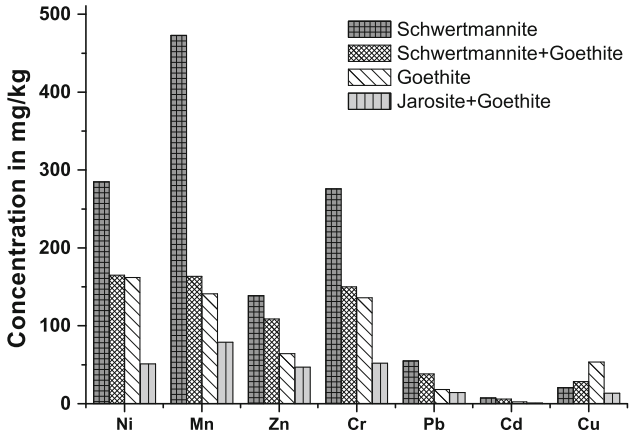

Fig. 5 Concentrations of elements in ochreous precipitates: schwertmannite (O-1), schwertmannite + goethite (O-2), goethite (O-3) and jarosite + goethite (O-5)

be less significant in controlling metal sorption onto Fe-precipitates, though it should be noted that the sorption of a particular metal onto the Fe-oxyhydroxide can be hindered by other dissolved constituents (Dzombak and Morel 1990; Kairies et al. 2005).

The Mn concentration was higher in one water sample (W-5); however, the concentration of Mn in the corresponding ochre sample (O-5) was less than that of other samples (Table 2). This ochre sample contains jarosite and has a low sorption affinity on the basis of CR values for various trace metals (Table 3). Mn sorption onto the ochre (O-5) might have been limited due to ferrous-ferric equilibrium (Hem 1977), wherein inhibition of Mn oxidation occurs in the presence of high levels of dissolved Fe^{2+} in the water (W-5). On the other hand, a high concentration of Mn was observed in the ochre (O-1), where the corresponding water sample had low Fe^{2+} but high Fe^{3+}. Hem (1964) reported a decreasing concentration of Fe^{2+} leading to the precipitation of Fe-oxides, with corresponding decreases in Mn and other dissolved metals. Similar observations were reported by Kairies et al. (2005).

Metal Fractionation

Metals in ochreous precipitates are known to exist in various forms (Kairies et al. 2005). Since the total concentration of metals does not necessarily correlate with the bioavailability of metals, a multi-step sequential extraction procedure was used to estimate the distribution of metals in Fe-oxyhydroxysulfate precipitates (Kairies 2003). Partitioning of metals into each fraction is presented in Fig. 6.

Soluble and exchangeable fractions of metals are more bioavailable, being loosely bound to the surface, and therefore are easily released, which may cause deleterious effects to the aqueous environment (Tessier et al. 1979). Except for Mn (9.5 %) and Cd (7.8 %), metals such as Fe (0.14 %), Ni (4.9 %), Cr (1.8 %), Zn (5.7 %), Pb (3.7 %), and Cu (3.2 %) are less associated with the bioavailable fractions. Major proportions (74–97 %) of all metals are associated with Fe oxide and hydroxide phases in the precipitates, indicating their possible adsorption on the Fe oxide structures and later incorporation into the structure (Cornell and Schwertmann 1996). Because of the high binding capacity of Fe(III) oxide/oxyhydroxide structures, these metals do not easily exchange with the aqueous phase, unless the environment (Eh, pH) is changed substantially to favor the dissolution of Fe-oxides (Cornell and Schwertmann 1996). In addition, about 8–12 % of the Ni, Zn, Cd, and Pb were partitioned into Mn oxide/hydroxide phases. Less than 4 % of the elements in all of the ochres were associated with organic and sulfide fractions. The above partitioning behavior of metals suggests that Fe oxyhydroxide phases, along with minor amounts of Mn oxide and hydroxide phases, play a major role in controlling mobility of metals in water affected by AMD from coal mines.

Conclusions

Fe-oxyhydroxide precipitates from AMD in the Jaintia coalfield are mainly composed of schwertmannite, goethite, and jarosite. These precipitates formed under acidic conditions and scavenged metals from the aqueous phase. Schwertmannite-bearing precipitates contain higher concentrations of metals than the goethite- and jarosite-bearing precipitates. Sorption of metals in ochreous precipitates is controlled by the surface area, crystallinity, and

Table 3 Concentration ratio (log CR) of the metals in ochreous precipitates compared to stream water

ID	Al	Fe	Ni	Mn	Cr	Pb	Cu	Cd	Zn	Sorption affinity order
O-1	3.2	4.1	3.9	3.0	5.1	3.3	3.5	3.1	4.0	Cr > Fe > Zn > Ni > Cu > Pb > Al > Cd > Mn
O-2	3.6	4.3	3.6	2.3	5.0	4.0	4.3	3.0	3.5	Cr > Fe ≈ Cu > Pb > Al ≈ Ni > Zn > Cd > Mn
O-3	3.0	4.3	3.1	2.2	4.5	2.4	3.4	2.4	2.2	Cr > Fe > Cu > Ni > Al > Pb ≈ Cd > Zn > Mn
O-4	3.0	4.0	3.5	2.4	4.5	3.2	3.9	1.4	3.6	Cr > Fe > Cu > Zn > Ni > Pb > Al > Mn > Cd
O-5	3.2	3.7	2.2	1.7	3.9	2.4	2.4	2.0	1.8	Cr > Fe > Al > Cu ≈ Pb > Ni > Cd > Zn > Mn

CR concentration ratio

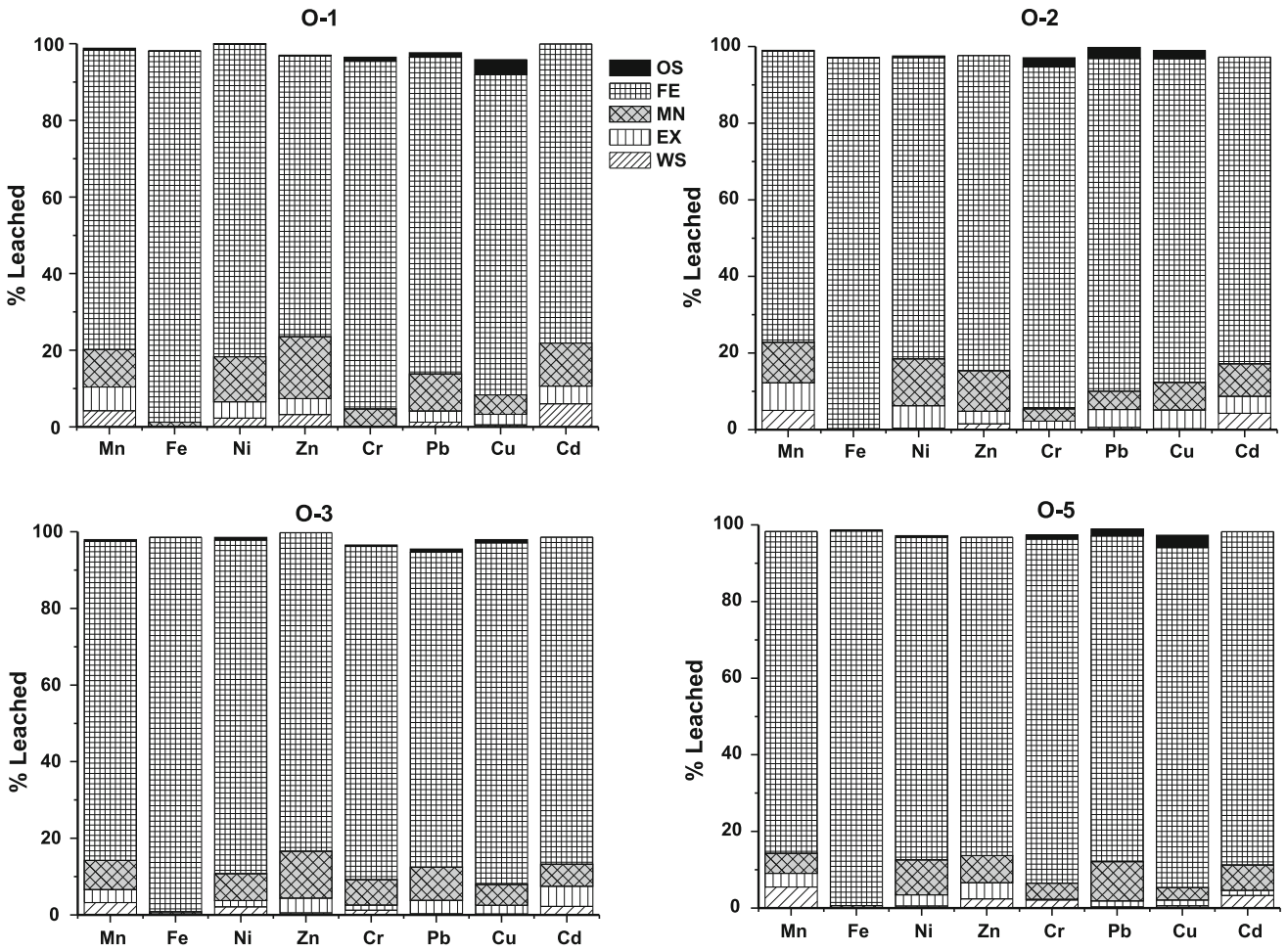

Fig. 6 Partitioning of metals in ochres collected from Jaintia Hills coalfield (*WS* water soluble, *EX* exchangeable and carbonate, *MN* manganese bound, *FE* iron bound, *OS* organic and sulfide bound)

concentrations of ions such as Fe^{2+}, Fe^{3+}, and Mn. Geochemical partitioning of metals revealed that Fe and Mn oxides/hydroxide phases in ochres play a major role in retention of metals from AMD-contaminated water bodies.

Acknowledgments PKS thanks the Indian Institute of Technology Kharagpur for financial assistance in the form of a research fellowship. Instrumental support for ICP-MS analysis was made available through the FIST Program of the Department of Science and Technology, Government of India to the Department of Geology and Geophysics, IIT Kharagpur. PKS is also thankful to Professor K. Kim of Kunsan National University for his helpful support and guidance. We are grateful to the editor and two anonymous reviewers for their constructive comments and suggestions that greatly improved the manuscript.

References

Acero P, Ayora C, Tottentó C, Nieto JM (2006) The behavior of trace elements during schwertmannite precipitation and subsequent transformation into goethite and jarosite. Geochim Cosmochim Acta 70:4130–4139

Ahmed M, Bora JP (1981) Geochemistry of tertiary coal, Bapung coalfield, Jaintia Hills, Meghalaya. J Assam Sci Soc 24:1–5

Ali MA, Dzombak DA (1996) Interactions of copper, organic acids, and sulfate in goethite suspensions. Geochim Cosmochim Acta 60:5045–5053

APHA (American Public Health Association) (1995) Standard methods for the examination of water and wastewater, 19th edn. APHA, Washington, DC

Bigham JM, Nordstrom DK (2000) Iron and aluminum hydroxysulfates from acid sulfate water. In: Alpers CN, Jambor JL, Nordstrom DK (eds) Sulfate minerals, crystallography, geochemistry, and environmental significance, Reviews in mineralogy and geochemistry, vol 40. Mineralogical Society of America and Geochemical Society, Washington, pp 351–403

Bigham JM, Schwertmann U, Carlson L, Murad E (1990) A poorly crystallized oxyhydroxysulfate of iron formed by bacterial oxidation of Fe (II) in acid mine water. Geochim Cosmochim Acta 54:2743–2758

Bigham JM, Schwertmann U, Traina SJ, Winland RL, Wolf M (1996) Schwertmannite and the chemical modeling of iron in acid sulfate waters. Geochim Cosmochim Acta 60:2111–2121

Brunauer S, Emmett PH, Teller E (1938) Adsorption of gases in multimolecular layers. J Am Chem Soc 60:309–315

Burton ED, Bush RD, Sullivan LA, Mitchell DRG (2007) Reduction transformation of iron and sulfur in schwertmannite-rich

accumulations associated with acidified coastal lowlands. Geochim Cosmochim Acta 71:4456–4473
Carlson L, Bigham JM, Schwertmann U, Kyek A, Wagner F (2002) Scavenging of As from acid mine drainage by schwertmannite and ferrihydrite: a comparison with synthetic analogues. Environ Sci Tech 36:1712–1719
Chandra D, Mazumdar K, Basumallick S (1983) Distribution of sulfur in the tertiary coals of Meghalaya, India. Int J Coal Geol 3:63–75
Cornell RM, Schwertmann U (1996) The iron oxides: structure, properties, reactions, occurrences and uses. VCH, Weinheim
Davis JA, Kent DB (1990) Surface complexation modeling in aqueous geochemistry. Miner Water Interface Geochem 23:177–260
Dzombak DA, Morel FMM (1990) Surface complexation modeling: hydrous ferric oxide. Wiley, New York
Equeenuddin Sk Md, Tripathy S, Sahoo PK, Panigrahi MK (2010) Geochemistry of ochreous precipitates from coal mine drainage in India. Environ Earth Sci 61:723–731
Gagliano WB, Brill MR, Bigham JM, Jones FS, Traina SJ (2004) Chemistry and mineralogy of ochreous sediments in a constructed mine drainage wetland. Geochim Cosmochim Acta 68:2119–2128
Gammons CH, Duaime TE, Parker SR, Poulson SR, Kennelly P (2010) Geochemistry and stable isotope investigation of acid mine drainage associated with abandoned coal mines in central Montana, USA. Chem Geol 269:100–112
Hem JD (1964) Deposition and solution of manganese oxides. USGS Water-Supply Paper 1667-B, Washington DC, USA
Hem JD (1977) Reactions of metals ions at surfaces of hydrous iron oxide. Geocheim Cosmochim Acta 41:527–538
Jönsson J, Persson P, Sjöberg S, Lövgren L (2005) Schwertmannite precipitated from acid mine drainage: phase transformation, sulfate release and surface properties. Appl Geochem 20:179–191
Kairies CL (2003) Characterization of precipitates associated with bituminous coal mine drainage, northern Appalachian region, USA, PhD Dissertation, University of Pittsburgh, PA, USA
Kairies CL, Capo RC, Watzlaf GR (2005) Chemical and physical properties of iron hydroxide precipitates associated with passive treated coal mine drainage in Bituminous Region of Pennsylvania and Maryland. Appl Geochem 20:1445–1460
Kim JJ, Kim SJ, Lee SS (2003) *Gallionella ferruginea* in ochreous precipitates from acid mine drainage in Gonghae coal mine area, Korea. Geosci J 7:289–292
Kleinmann RLP, Crerar DA, Pacelli RP (1981) Biogeochemistry of acid mine drainage and a method to control acid formation. Mining Eng 33:300–305
Lazaroff N, Sigal W, Wasserman A (1982) Iron oxidation and precipitation of ferric hydroxysulfates by resting *Thiobacillus ferrooxidans* cells. Appl Environ Microb 43:924–938
Lee G, Bigham JM, Faure G (2002) Removal of trace metals by coprecipitation with Fe, Al, and Mn from natural waters contaminated with acid mine drainage in the Ducktown Mining District, Tennessee. Appl Geochem 17:569–581
Lu P, Nuhfer NT, Kelly S, Li Q, Konishi H, Elswick E, Zhu C (2011) Lead coprecipitation with oxyhydroxide nano-particles. Geochim Cosmochim Acta 75:4547–4561
Munk LA, Faure G, Pride DE, Bigham JM (2002) Sorption of trace metals to an aluminum precipitate in a stream receiving acid rock-drainage; Snake River, Summit County, Colorado. Appl Geochem 17:421–430
Murad E, Rojik P (2003) Iron-rich precipitates in a mine drainage environment: influence of pH on mineralogy. Am Mineral 88:1915–1918
Regenspurg S, Peiffer S (2002) A FTIR spectroscopical study to explain bonding structures of arsenate and chromate associated with schwertmannite. In: Schulz HD, Hadeler A (eds) Geochemical processes in soil and groundwater. Wiley-VCH, New York, pp 78–92
Rose AW, Bianchi-Mosquera G (1993) Adsorption of Cu, Pb, Zn, Co., Ni, and Ag on goethite and hematite: a control on metal mobilization from red beds into stratiform copper deposits. Econ Geol 88:1226–1236
Ryskin YI (1974) The vibrations of protons in minerals: hydroxyl, water and ammonium. In: Farmer VC (ed), The infrared spectra of minerals. Mineral Soc Monograph 4:137–182
Sahoo PK, Tripathy S, Equeenuddin SkMd, Panigrahi MK (2012) Geochemical characteristics of coal mine discharge vis-à-vis behavior of rare earth elements at Jaintia Hill Coalfield, Northeastern India. Gechem Explor 112:235–243
Saikia BJ, Parthasarathy G (2010) Fourier transform infrared spectroscopic characterization of kaolinite from Assam and Meghalaya, Northeastern India. Mod Phys 1:206–210
Schroth AW, Parnell RA Jr (2005) Trace metal retention through the schwertmannite to goethite transformation as observed in a field setting, Alta Mine, MT. Appl Geochem 20:907–917
Schwertmann U (1964) Differenzierunrr der Eisenoxide des Bodens durch photochemische Extraktion mit saurer Ammoniumoxalat-Losung. Z Pflanzen Bodenkunde 105:194–202
Schwertmann U, Carlson L (2005) The pH-dependent transformation of schwertmannite to goethite at 25 °C. Clay Miner 40:63–66
Sidenko NV, Sherriff BL (2005) The attenuation of Ni, Zn and Cu, by secondary Fe phases of different crystallinity from surface and groundwater of two sulfide mine tailings in Manitoba, Canada. Appl Geochem 20:1180–1194
Singh MP, Singh AK (2000) Petrographic characteristics and depositional conditions of eocene coals of platform basins, Meghalaya, India. Int J Coal Geol 42:315–356
Swer S, Singh OP (2003) Coal mining impacting water quality and aquatic biodiversity in Jaintia Hills district. ENVIS Bull Himalaya Ecol 11:25–33
Tessier A, Campbell PGC, Bisson M (1979) Sequential extraction for the speciation of particular trace metals. Anal Chem 363: 594–595
Webster JG, Swedlund PJ, Webster KS (1998) Trace metal adsorption onto acid mine drainage iron(III) oxy hydroxyl sulfate. Environ Sci Tech 32:1361–1368
Wedepohl KH (1995) The composition of the continental crust. Geochim Cosmochim Acta 59:1217–1232
Xu CY, Schwartz FW, Traina SJ (1997) Treatment of acid-mine water with calcite and quartz sand. Environ Eng Sci 14:141–152